

SIGNALLING

Class 3 phosphoinositide 3-kinase promotes hepatic glucocorticoid receptor stability and transcriptional activity

Yui Shibayama^{1,2,3,4} | Chantal Alkhoury^{1,2,3} | Ivan Nemazanyy⁵  |
 Nathaniel F Henneman^{1,2,3} | Nicolas Cagnard⁶ | Muriel Girard^{1,2,3,7} |
 Tatsuya Atsumi⁴ | Ganna Panasyuk^{1,2,3} 

¹Institut Necker-Enfants Malades (INEM), Paris, France

²INSERM U1151/CNRS UMR 8253, Paris, France

³Université de Paris, Paris, France

⁴Department of Rheumatology, Endocrinology and Nephrology, Faculty of Medicine and Graduate School of Medicine, Hokkaido University, Sapporo, Japan

⁵Platform for Metabolic Analyses, Structure Fédérative de Recherche Necker, INSERM US24/CNRS UAR 3633, Paris, France

⁶Bio-Informatique Platform, Structure Fédérative de Recherche Necker, INSERM US24/CNRS, UAR 3633, Paris, France

⁷Pediatric Hepatology Unit, Hôpital Necker-Enfants Malades, Assistance Publique-Hôpitaux de Paris, Paris, France

Correspondence

G. Panasyuk, Laboratory of Nutrient Sensing Mechanisms, Inserm U1151/CNRS UMR 8253, Institute Necker-Enfants Malades (INEM), 156-160 Rue de Vaugirard, Paris 75015, France.
Email: ganna.panasyuk@inserm.fr

Funding information

H2020 European Research Council, Grant/Award Number: ERC-2018-CoG-819543; Agence Nationale de la Recherche, Grant/Award Number: ANR-JCJC-NUTRISENSPIK-16-CE14-0029

Abstract

Aim: Lipid kinase class 3 phosphoinositide 3-kinase (PI3K) and nuclear receptor transcription factor glucocorticoid receptor (GR) play essential physiological roles in metabolic adaptation to fasting by activating lysosomal degradation by autophagy and metabolic gene expression, yet their functional interaction is unknown. The requirement of class 3 PI3K for GR function was investigated in liver tissue.

Methods: Inactivation of class 3 PI3K was achieved through deletion of its essential regulatory subunit Vps15, by expressing Cre-recombinase in the livers of Vps15^{f/f} mice. The response to both 24-h fasting and synthetic GR ligand, dexamethasone (DEX) was evaluated in control and mutant mice. Liver tissue was analysed by immunoblot, RT-qPCR, and LC-MS.

Results: Vps15 mutant mice show decreased transcript levels of GR targets, coupled with lower nuclear levels of total and phosphorylated on Ser211, GR protein. Acute DEX treatment and 24-h fasting both failed to re-activate expression of GR targets in the livers of Vps15 mutant mice to the levels observed in controls. Decreased levels of endogenous GR ligand corticosterone and lower expression of 11 β -hydroxysteroid dehydrogenase 1 (11 β -HSD1), a metabolic enzyme that controls corticosterone availability, were found in the livers of Vps15 mutants. Hepatic Vps15 depletion resulted in the activation of nuclear Akt1 signalling, which was paralleled by increased polyubiquitination of GR.

Conclusion: In the liver, class 3 PI3K is required for corticosterone metabolism and GR transcriptional activity.

KEYWORDS

Akt signalling, class 3 phosphoinositide 3-kinase, corticosterone, glucocorticoid receptor, liver

See related editorial: Jacobi D. 2022. Old pathways –New crossroads: Class 3 PI3K acts on glucocorticoid signal transduction *Acta Physiol (Oxf)*. e13812.

This is an open access article under the terms of the Creative Commons Attribution-NonCommercial-NoDerivs License, which permits use and distribution in any medium, provided the original work is properly cited, the use is non-commercial and no modifications or adaptations are made.

© 2022 The Authors. *Acta Physiologica* published by John Wiley & Sons Ltd on behalf of Scandinavian Physiological Society.

1 | INTRODUCTION

Hormone-activated nutrient-sensing signal transduction pathways control gene expression networks that are required for metabolic adaptation in response to energy availability. Multiple functional interactions were reported between pro-anabolic insulin stimulated class 1 phosphoinositide 3-kinase (PI3K) and pro-catabolic steroid-induced glucocorticoid receptor (GR) transcription factor.¹⁻⁵ However, crosstalk between GR and the pro-catabolic branch of PI3K family, class 3 PI3K, was never addressed. Class 3 PI3K is critical for cellular processes of endocytic trafficking, autophagy, and lysosomal activity via synthesis of lipid second messenger phosphatidylinositol-3 phosphate (PI3P).^{6,7} Class 3 PI3K functions as an obligate complex of regulatory Vps15 and catalytic Vps34 subunits.⁶ We and others have demonstrated that class 3 PI3K contributes to metabolic homeostasis by limiting insulin receptor and Akt signalling in physiology.^{8,9} The latter is manifested by increased phosphorylation of Akt substrates such as Forkhead box protein O1 (FoxO1) transcription factor, and metabolic alterations including defective gluconeogenesis in hepatic mutants of class 3 PI3K.⁸ Moreover, in fasting, class 3 PI3K plays an essential role in fatty acid oxidation and mitochondrial biogenesis by controlling selective autophagy of transcriptional repressors Nuclear Receptor Corepressor 1 (NCoR1) and Histone Deacetylase 3 (Hdac3).^{10,11} An accumulation of these transcriptional repressors in the livers of autophagy mutants manifests in the inhibition of transcription factor Peroxisome proliferator-activated receptor alpha (PPAR α), a master regulator of lipid catabolism. Although these findings advocate an important role of class 3 PI3K for transcriptional responses in fasting, its requirement for an effective GR transcriptional program is not known.

Glucocorticoids (GCs) are steroid hormones secreted from the adrenal gland, release of which is controlled by the stress-responsive hypothalamic-pituitary-adrenal (HPA) system.¹² Systemic GCs act in hepatocytes by binding to GR to promote its activation.¹³ GC-activated GR acts as a homo- or heterodimer with other transcription factors such as PPAR α to inhibit inflammatory gene expression and to induce gluconeogenesis and lipid metabolism.^{12,14,15} However, excessive activation of GR in the liver could inflict undesirable metabolic effects such as induction of lipid synthesis; thus, it is tightly controlled at multiple levels.^{12,16-18} First, the balance between expression of active GR α and inhibitory GR β isoform is maintained by alternative splicing.¹⁹ Second, GR protein turnover by proteasomal degradation is controlled by post-translational modifications, including phosphorylation downstream of insulin-activated Akt signalling.²⁰ Third, its nuclear translocation and nuclear retention are

impacted by binding to heat shock proteins.^{21,22} Finally, GR ligand levels in hepatocytes are controlled by 11 β -hydroxysteroid dehydrogenase-1 (11 β HSD1), an enzyme that converts inactive 11-Dehydrocorticosterone to its active form, corticosterone.^{23,24}

Although GR could transcriptionally activate autophagy,²⁵⁻²⁷ the role of class 3 PI3K upstream of GR is not reported. Here, we show that class 3 PI3K is essential for GR function in the liver of mice both during physiological fasting (middle of the day) and prolonged 24-h starvation. Inactivation of class 3 PI3K by deleting its essential regulatory subunit, Vps15, results in defective GR transcriptional responses. First, liver-specific deletion of Vps15 manifested in lower expression of GR target genes. Second, in the livers of Vps15 mutants, both fasting and DEX treatment did not induce expression of GR targets to the levels observed in control mice. This defect was mirrored by decreased phosphorylation of nuclear GR on Ser211; the residue crucial for its transcriptional activity. Third, deletion of Vps15 resulted in significantly lower hepatic levels of GR ligand, corticosterone, without impacting its circulating levels in plasma. Finally, we show that polyubiquitinated GR is accumulated in hepatic mutants of Vps15, consistent with increased nuclear Akt1 signalling and activation of Mouse double minute 2 homolog (Mdm2) E3 ligase. Altogether, these findings place class 3 PI3K upstream of GR transcriptional activity in the liver.

2 | RESULTS

2.1 | Inhibited GR transcriptional activity in Vps15-null liver

To test if hepatic class 3 PI3K has a role in GR-driven transcriptional responses, we performed comparative analyses of differentially expressed genes in published microarray sets of liver tissues from GR¹⁹ and Vps15 mutants.¹⁰ Notably, although these transcriptomic data sets were generated independently, they were performed with internal controls allowing the filtering of differentially expressed genes. These analyses demonstrated that transcript levels of 3901 and 2120 unique genes were modified more than 1.2-fold compared with internal controls in Vps15-LKO and GR-LKO respectively (Figure 1A). Intersection of differentially expressed genes revealed 443 genes that were common in both data sets (Figure 1A). The findings of 443 genes among 3901 of all differentially expressed genes in Vps15-LKO mice suggested that class 3 PI3K might act upstream of GR transcriptional factor function. Among these 443 shared genes, 350 genes (79%) were co-regulated similarly in both mutants with 139 genes of 350 were downregulated, whereas 211 genes of 350 were

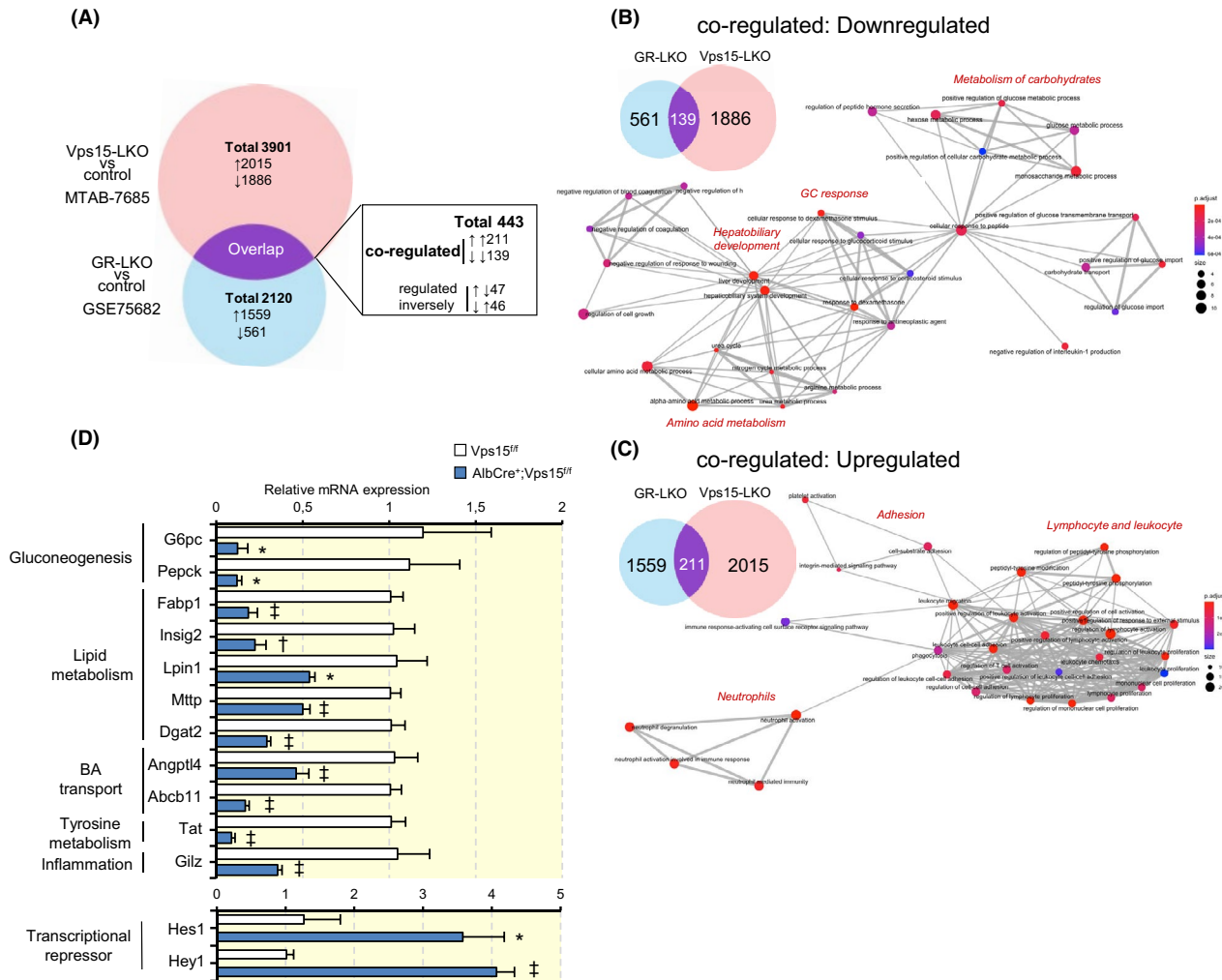


FIGURE 1 Repressed transcriptional activity of GR in hepatic mutants of Vps15. A, Venn diagram showing the overlap of the differentially expressed genes in the liver in microarray sets of GR-LKO (GSE75682) and Vps15-LKO (MTAB-7685) mice. The numbers of unique genes modified above 1.2-fold in each microarray and overlap between two data sets are shown. Functional clustering analysis of significantly enriched biological processes by DAVID-GO for co-regulated genes (downregulated (B) or upregulated (C)) in the livers of GR-LKO and in Vps15-LKO mice. D, Transcript levels by RT-qPCR of GR target genes functioning in different processes. The liver tissue of random-fed, 6-week-old Vps15^{f/f} and AlbCre⁺; Vps15^{f/f} mice was collected in the middle of the day corresponding to physiological fasting period. Data are means ± SEM (n = 4 for Vps15^{f/f}, n = 4 for AlbCre⁺; Vps15^{f/f}, *P < .05, †P < .01, ‡P < .001: vs Vps15^{f/f} mice, two-tailed, unpaired Student's *t* test)

upregulated. The subsequent Gene Ontology (GO) pathway analyses among the co-regulated downregulated genes showed a significant enrichment of 30 biological processes (Figure 1B). As expected, those encompassed processes clustered around response to DEX, amino acid and glucose metabolism, and more generally, liver and hepatobiliary system development (Figure 1B). Moreover, consistent with GR's role in repressing inflammation, GO pathway analyses of genes upregulated in both mutants highlighted the processes of immune cell activation, migration and proliferation (leukocytes, neutrophils, T-cells, mononuclear cells) (Figure 1C).

Next, to validate these observations of transcriptional analyses, we used liver-specific Vps15-deficient

AlbCre⁺; Vps15^{f/f} mice, hereafter referred to as Vps15-LKO.⁸ Notably, analyses by real-time quantitative PCR (RT-qPCR) in the livers of Vps15-LKO mice, further supported initial observations of GR inhibition upon class 3 PI3K inactivation in the liver (Figure 1D). To this end, significantly decreased transcript levels in the livers of Vps15-LKO mice were detected for *bona fide* gene targets of GR in gluconeogenesis (*G6pc*, *Pepck*), lipid metabolism (*Fabp1*, *Insig2*, *Lpin1*, *Mttp*, *Dgat2*), bile acid transport (*Angptl4*, *Abcb11*), tyrosine metabolism (*Tat*) and inflammation (*Gilz*). Moreover, consistently with the repressive role of GR for their transcription, the transcript levels of *Hes1* and *Hey1* were significantly increased in the liver of Vps15-LKO mice (Figure 1D). Altogether, these findings

suggest that GR is inhibited in the livers of Vps15-LKO mice.

2.2 | Decreased nuclear expression of GR in Vps15-null liver

Given the findings of decreased transcript levels of GR targets genes, we asked if inactivation of class 3 PI3K impacts GR protein expression. As we reported earlier, hepatic Vps15 depletion results in degradation of the lipid kinase, Vps34 protein.⁸ This leads to the severe inhibition of endocytic trafficking and lysosomal degradation by autophagy, witnessed by significant accumulation of lysosomal membrane protein Lamp2, autophagy receptor p62 and autophagosome-associated protein LC3-II (Figure 2A). These defects in proteostasis in the livers of Vps15-LKO mice were accompanied by significantly decreased GR protein levels (Figure 2A). Of note, the anti-GR antibody that we used recognizes both GR α and GR β splicing isoforms that differ only in 15aa. Notably, GR β does not bind to GC and also is reported to act as an inhibitor of GR α transcriptional activity.²⁸ In physiology, the expression of GR β in the liver is low, with GR α acting as a predominant isoform of GR in this tissue. The lack of compensatory GR β overexpression in Vps15-LKO mice was demonstrated by RT-qPCR analyses using isoform discriminating primer pairs. In line with decreased protein expression of GR, we found lower levels of GR α isoform and unmodified GR β transcript levels in Vps15-LKO mice (Figure 2B). Next, given that GR phosphorylation on Ser211 is the mark of its transcriptional activity in response to GCs,²⁹ we analysed the phosphorylation of GR in Vps15-LKO mice. Consistent with lower levels of GR total protein, the levels of its phosphorylated on Ser211 form were significantly decreased in the livers of Vps15-LKO mice (Figure 2A). Of note, the quantification of phosphorylated on Ser211 GR normalized to total GR levels showed similar ratio in the livers of control and Vps15-LKO mice further confirming that there is no compensatory hyper-phosphorylation of GR protein in Vps15 mutants. Furthermore, given the observations of decreased GR protein levels in total liver extracts of Vps15-LKO mice, we analysed the expression of GR and GR phosphorylated at Ser211 in nuclear fractions of the liver tissue. Consistent with findings in total protein extracts, significant depletion of GR and phosphorylated GR was observed in liver nuclear fractions of Vps15-LKO mice (Figure 2C). In sum, these transcript and protein expression analyses in the livers of Vps15 mutants suggest that class 3 PI3K acts upstream of GR by maintaining its nuclear expression and phosphorylation.

2.3 | Fasting and DEX treatment does not fully rescue GR target levels in Vps15-LKO mice

Next, we asked whether expression of GR targets in the livers of Vps15-LKO mice could be rescued by fasting or pharmacologically, by its synthetic agonist DEX. First, we tested the impact of fasting and for this, control and Vps15-LKO mice were killed at the onset of darkness (active feeding phase) with or without 24-h starvation. As seen from Figure 3A, in the livers of control mice, 24-h fasting induced the transcript levels of genes in gluconeogenesis (*G6pc*, *Pepck*) and in lipid metabolism (*Lpin1*, *Mttp*, *Insig2*). Notably, in line with transcriptomic analyses presented on Figure 1D, the expression of GR targets significantly decreased (increased for *Hey1*, consistent with the repressive role of GR for its expression) in the livers of Vps15-LKO mice. Although fasting did not fully rescue expression of GR-gene targets in Vps15-LKO mice to the levels observed in control mice (Figure 3A), the magnitude of changes in response to fasting was comparable between both genotypes for most targets with the exception of *Mttp* gene. Next, given these observations in fasting, we asked whether acute administration of potent GR agonist, DEX, for 5 h could fully restore its activity in the livers of Vps15 mutants. The transcript analyses by RT-qPCR showed that, in the livers of control mice, the majority of GR targets were responsive to short-term DEX administration (*Tat*, *Gilz*, *Lpin1*, *Insig2*, *Dgat2*, *Hey1*), except for the gluconeogenesis genes (*G6pc* and *Pepck*) (Figure 3B). Moreover, similar to fasting, acute DEX administration, did not rescue the transcript levels of GR targets in the livers of Vps15-LKO mice to the levels observed in controls (Figure 3B). Of note, the magnitude of responses to DEX treatment in the livers of Vps15 mutants was gene-dependent. The first group of responsive genes (*Lpin1*, *Gilz* and *Hey1* genes) showed similar magnitude of changes in both control and mutant mice, whereas in the second group (*Dgat2*, *Insig2* and *Tat* genes) it was lower in Vps15 mutants compared with control mice (Figure 3B). Furthermore, in agreement with its transcriptional inhibition, nuclear GR protein and its phosphorylated form on Ser211 were decreased in the livers of Vps15-LKO mice both in fasting and in response to DEX treatment (Figure 3C). Notably, the phosphorylation of GR on Ser211 was induced on DEX treatment in the livers of control mice, whereas it was unmodified in the livers of Vps15-LKO mice (Figure 3C). Altogether, neither fasting nor acute administration of DEX could restore the expression of GR target genes in the livers of Vps15-LKO mice to the levels of control mice.

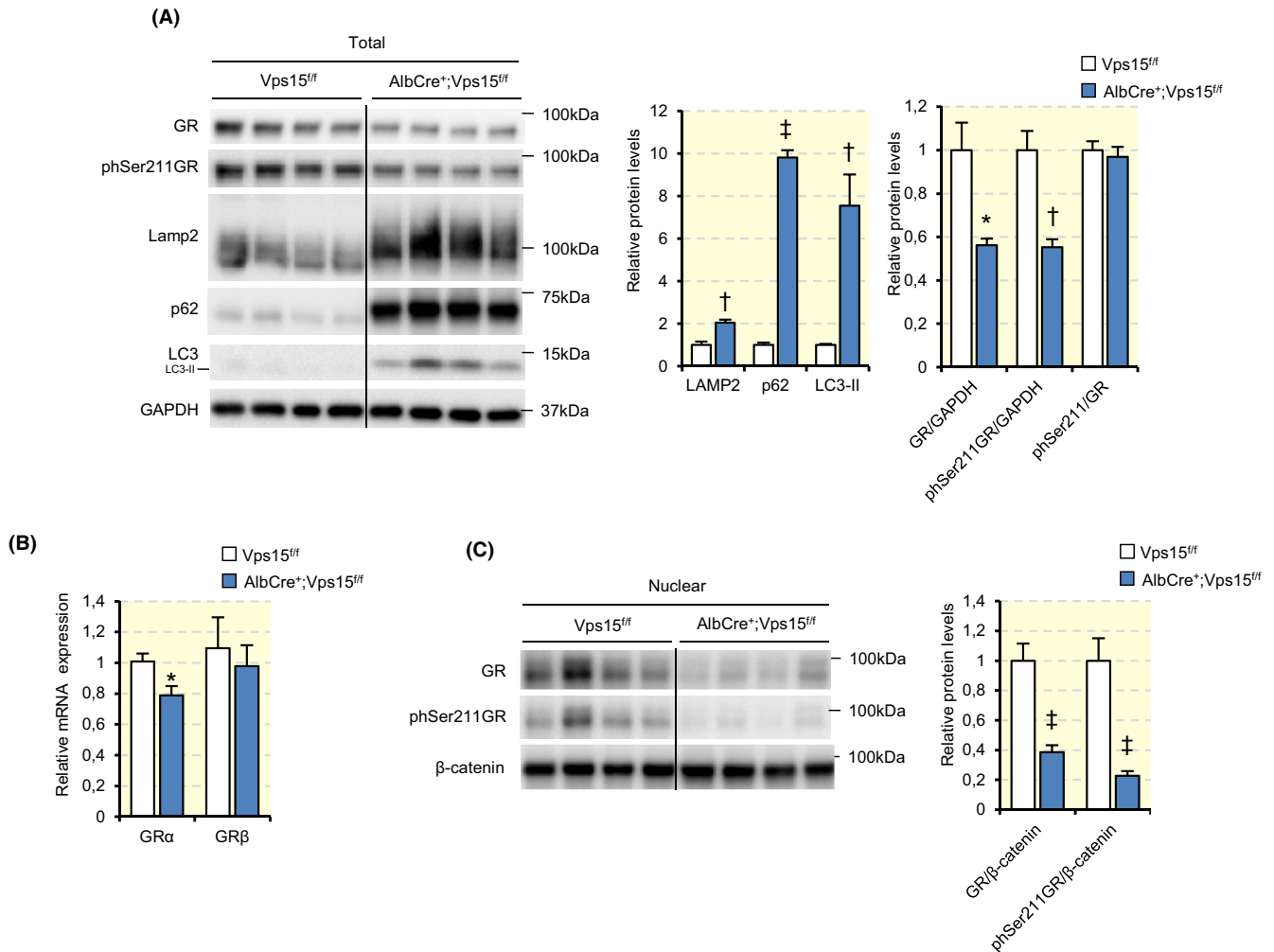


FIGURE 2 Decreased nuclear expression of GR in the livers of Vps15-LKO mice. A, Immunoblot analysis of total protein of liver extracts from random-fed, 6-week-old Vps15^{fl/fl} and AlbCre⁺; Vps15^{fl/fl} mice using indicated antibodies. The liver tissue was collected in the middle of the day corresponding to physiological fasting period. Immunoblot with anti-GAPDH antibody served as a loading control. Densitometric analyses of protein levels normalized to GAPDH levels presented as folds over Vps15^{fl/fl} mice. Data are means \pm SEM (n = 4 for Vps15^{fl/fl}, n = 4 for AlbCre⁺; Vps15^{fl/fl}, **P* < .05, †*P* < .01, ‡*P* < .001: vs Vps15^{fl/fl}, two-tailed, unpaired Student's *t* test). B, Relative transcript levels of GR isoforms, GR α and GR β in the livers of Vps15^{fl/fl} and AlbCre⁺; Vps15^{fl/fl} analysed by RT-qPCR (liver tissue collected as in (A)). Data are means \pm SEM (n = 8 for Vps15^{fl/fl}, n = 9 for AlbCre⁺; Vps15^{fl/fl}, **P* < .05: vs Vps15^{fl/fl} mice, two-tailed, unpaired Student's *t* test). C, Immunoblot analysis using indicated antibodies of nuclear fraction of liver extracts from Vps15^{fl/fl} and AlbCre⁺; Vps15^{fl/fl} mice (liver tissue collected as in (A)). Immunoblot with β -catenin antibody served as a loading control. Densitometric analyses of protein levels normalized to β -catenin levels presented as folds over Vps15^{fl/fl}. Data are means \pm SEM (n = 4 for Vps15^{fl/fl}, n = 4 for AlbCre⁺; Vps15^{fl/fl}, ‡*P* < .001: vs Vps15^{fl/fl}, two-tailed, unpaired Student's *t* test)

2.4 | Expression of nuclear co-regulators of GR is altered in Vps15-LKO

GR resides in the cytosol in a repressive complex with Hsp90 and Hsp70 chaperone proteins.^{22,30} To test whether the inhibition of GR observed in the livers of Vps15-LKO mice is associated with overexpression of the chaperones, we analysed their levels in total protein extracts. These immunoblot analyses showed that expression of Hsp70 is significantly decreased while levels of Hsp90 are not modified in the livers of Vps15-LKO mice (Figure 4A). Given that nuclear

Hsp90 was also reported to bind GR to repress its transcriptional activity,³¹ we next asked whether nuclear levels of Hsp90 are modified in Vps15-LKO mice. Immunoblot analyses of nuclear fractions showed significantly upregulated Hsp90 expression in the livers of Vps15-LKO mice compared with controls (Figure 4B). Recent BioRxiv pre-print study suggested that nuclear Fabp1 protein could act as a co-activator of GR, similarly to its effect on PPAR α ³² (<https://doi.org/10.1101/2021.07.02.450968>). Consistent with the inhibition of GR observed in Vps15-LKO mice, nuclear levels of Fabp1 were depleted in the livers of Vps15 mutant

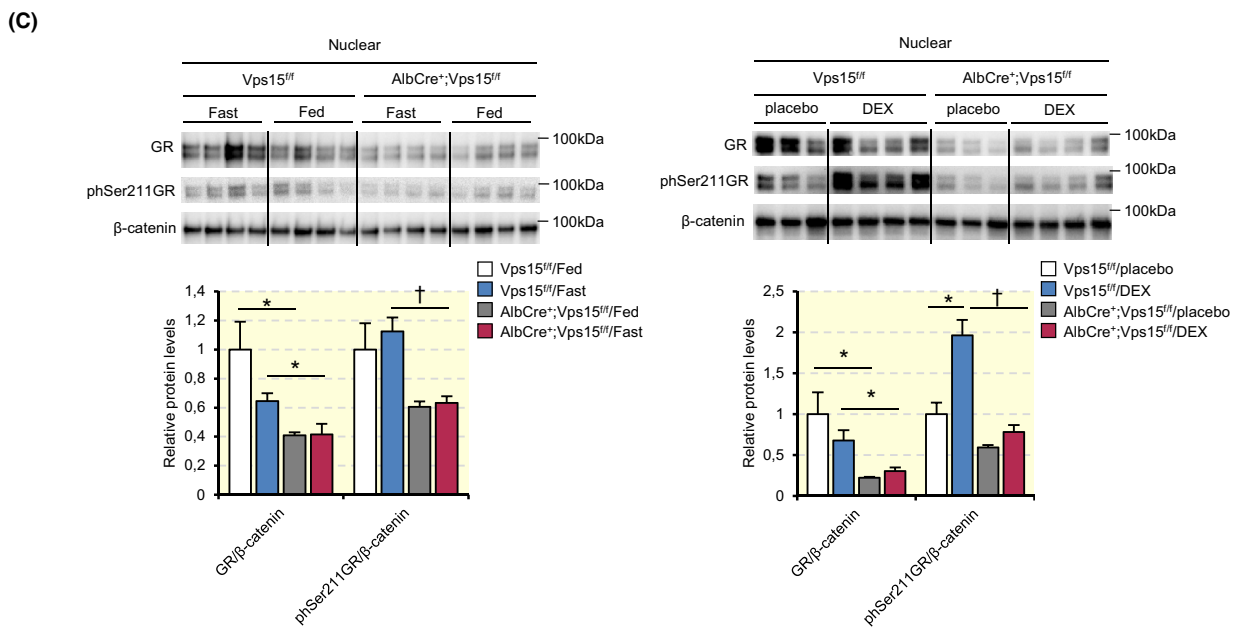
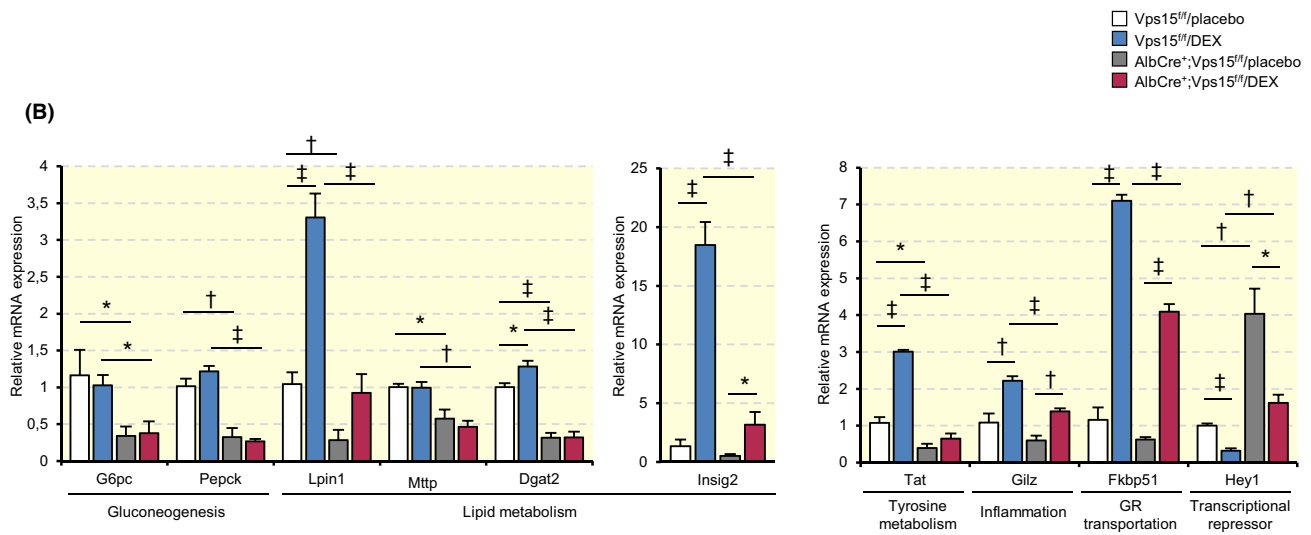
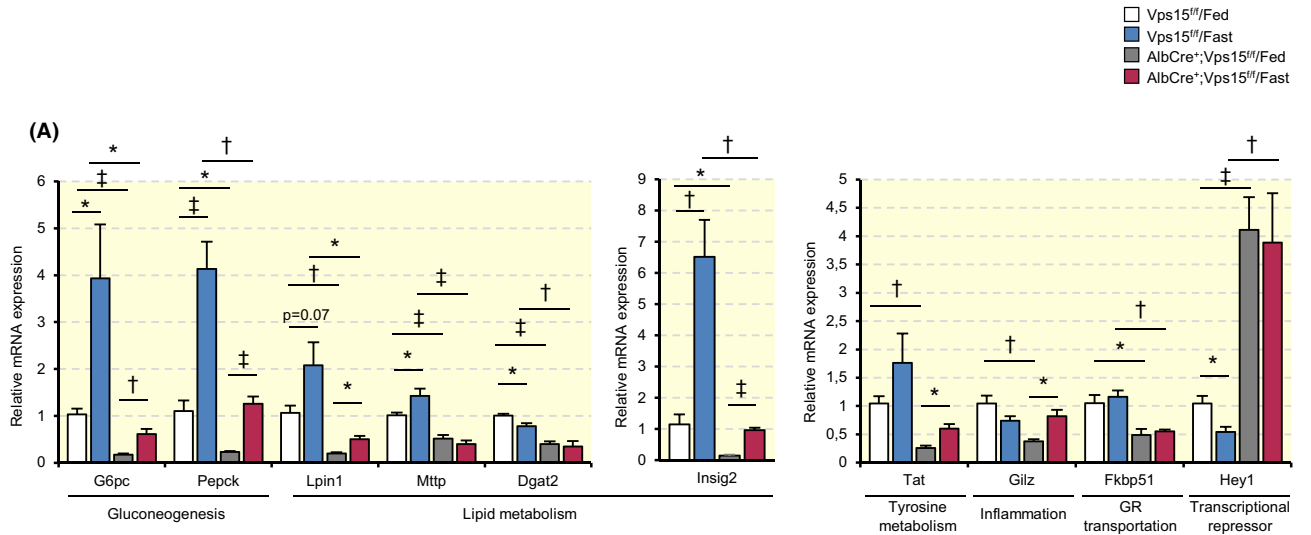


FIGURE 3 Incomplete reactivation of GR in the livers of Vps15-LKO mice in response to fasting and acute DEX treatment. **A**, Relative transcript levels of GR target genes in the livers of Vps15^{fl/fl} and AlbCre⁺; Vps15^{fl/fl} by RT-qPCR. The 6-week-old mice were fasted at the onset of night (active feeding period) and both treatment groups sacrificed 24 h after. Data are means \pm SEM (Vps15^{fl/fl} (n = 6 for fed and fast group), AlbCre⁺; Vps15^{fl/fl} (n = 4 and n = 5 for fed and fast group), **P* < .05, †*P* < .01, ‡*P* < .001: two-tailed, unpaired Student's *t* test). **B**, Relative transcript levels of GR target genes in the livers of Vps15^{fl/fl} and AlbCre⁺; Vps15^{fl/fl} mice by RT-qPCR. The 6-week-old mice were injected IP with DEX (50 mg/kg) at the onset of the day phase and liver tissue collected 5 h later (middle of the day corresponding to physiological fasting period). Data are means \pm SEM (Vps15^{fl/fl} (n = 4 for placebo and DEX group), AlbCre⁺; Vps15^{fl/fl} (n = 5 for placebo and DEX group), **P* < .05, †*P* < .01, ‡*P* < .001: two-tailed, unpaired Student's *t* test). **C**, Immunoblot analysis of nuclear extracts of the liver tissue collected under the conditions as in (A) and (B) using indicated antibodies. Densitometric analyses of protein levels normalized to β -catenin levels presented as folds over Vps15^{fl/fl}-placebo condition. Data are means \pm SEM (Vps15^{fl/fl} (n = 4 for fed and fast group), AlbCre⁺; Vps15^{fl/fl} (n = 4 for fed and fast group), Vps15^{fl/fl} (n = 3 and n = 4 for placebo and DEX group), AlbCre⁺; Vps15^{fl/fl} (n = 3 and n = 4 for placebo and DEX group), **P* < .05, †*P* < .01, two-tailed, unpaired Student's *t* test)

(Figure 4B). Altogether, these expression analyses suggest that class 3 PI3K might impact nuclear GR function through availability of its co-regulators.

2.5 | Metabolism of GC ligand in the liver is dependent on Vps15

GC availability is controlled by the activity of two cytosolic enzymes, 11 β -hydroxysteroid dehydrogenase (HSD1) and 11 β -hydroxysteroid dehydrogenase-2 (11 β HSD2).²⁴ In mice, 11 β HSD1 converts non-active GC, 11-dehydrocorticosterone, to its active form corticosterone. Inversely, corticosterone inactivation is mediated by 11 β -HSD2. 11 β HSD1 is highly expressed in the liver, while expression of 11 β HSD2 is limited to the kidney, colon and sweat gland.²⁴ To test whether the inhibition of GR transcriptional activity in the liver of Vps15-LKO mice could be due to changes in its ligand metabolism, we measured 11 β HSD1 transcript levels. Expression analyses showed that in line with GR inhibition, 11 β HSD1 transcript levels were significantly decreased in the livers of Vps15-LKO mice (Figure 4C). These findings were mirrored by decreased transcript levels of C/EBP α and C/EBP β , two transcription factors upstream of 11 β HSD1³³ (Figure 4C). Finally, in accordance with the findings of decreased 11 β HSD1 expression, hepatic corticosterone levels were reduced in the livers of Vps15 mutants (Figure 4D). Of note, corticosterone levels in plasma were not different between Vps15-LKO and control mice, ruling out defects of its secretion from adrenal glands (Figure 4D). In sum, inhibition of GR is accompanied by decreased availability of its ligand in the livers of Vps15-LKO mice.

2.6 | Acute depletion of Vps15 in the liver results in GR inhibition

Next, we asked to which extent GR inhibition in Vps15-LKO mice could be reproduced by acute depletion of

Vps15 in the liver. For this, we transduced Vps15^{fl/fl} mice with adenoviral vectors expressing CRE-recombinase or, as a control, GFP protein and collected the liver tissue 10 days after transduction. In our previous study, we validated the selectivity and effectiveness of this acute approach for class 3 PI3K inactivation in the livers of adult mice.⁸ Similar to chronic inactivation of class 3 PI3K, acute depletion of Vps15 led to decreased transcript levels of numerous GR gene targets (Figure S1A). However, comparing the magnitude of decrease in these two conditions, the acute depletion of Vps15 was less potent (compare Figure 1D and Figure S1A). This is illustrated by the tendency to decrease of *Insig2*, *Tat* and *Gilz* transcript levels. Notably, both acute and chronic depletion of Vps15 manifested in profound defects of autophagy, witnessed by similar magnitude of p62 protein accumulation (Figure 2A and Figure S1B). Unlike on chronic inactivation, protein levels of GR and its form phosphorylated on Ser211 were largely unmodified by acute Vps15 depletion (minor decrease in phosphorylated form of GR upon Vps15 depletion was significant) (Figure S1B). Furthermore, acute loss of Vps15 did not lead to significant changes in protein levels of chaperones Hsp70 or Hsp90 (Figure S1B). As in Vps15-LKO mice, acute inactivation of Vps15 led to a decrease in transcript levels of 11 β HSD1; however, it did not significantly impact transcript levels of C/EBP β (Figure S1C). Finally, these expression changes were accompanied by a tendency to decrease of corticosterone levels in the livers of mice with acute Vps15 depletion (Figure S1D). Overall, these findings in mice upon acute deletion of Vps15 suggest an inhibition of GR transcriptional activity without impacting its protein levels.

2.7 | Increased ubiquitination of GR in the livers of Vps15-LKO mice

To gain further insights into mechanisms of GR dysfunction upon chronic inactivation of class 3 PI3K, we asked whether it could be because of its repression by activated

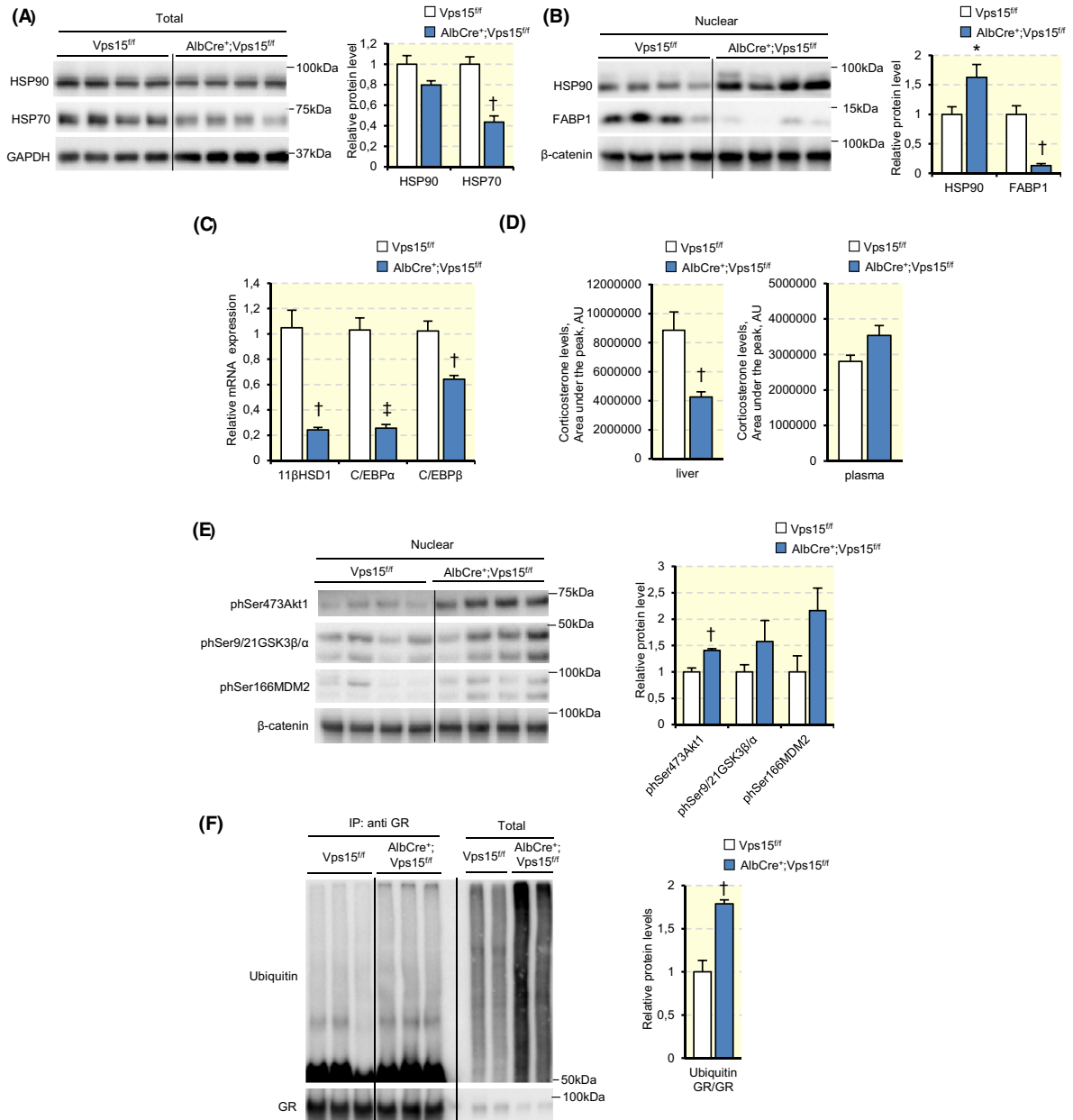


FIGURE 4 Decreased corticosterone levels and increased GR polyubiquitination in the livers of Vps15-LKO mice. A, Immunoblot analysis of total protein extracts of the liver tissue of random-fed, 6-week-old Vps15^{f/f} and AlbCre⁺; Vps15^{f/f} using indicated antibodies. The liver tissue was collected in the middle of the day corresponding to the physiological fasting period. Densitometric analyses of protein levels normalized to GAPDH protein levels presented as folds over Vps15^{f/f}. Data are means ± SEM (n = 4 for Vps15^{f/f}, n = 4 for AlbCre⁺; Vps15^{f/f}, †P < .01; vs Vps15^{f/f}, two-tailed, unpaired Student's *t* test). B, Immunoblot analysis of nuclear extracts of the liver tissue collected as in (A) using indicated antibodies. Densitometric analyses of protein levels normalized to β-catenin levels presented as folds over Vps15^{f/f}. Data are means ± SEM (n = 4 for Vps15^{f/f}, n = 4 for AlbCre⁺; Vps15^{f/f}, †P < .01; vs Vps15^{f/f}, two-tailed, unpaired Student's *t* test). C, Relative transcript levels of 11βHSD1, C/EBPα, and C/EBPβ in the livers Vps15^{f/f} and AlbCre⁺; Vps15^{f/f} mice collected as in (A) analysed by RT-qPCR. Data are means ± SEM (n = 6 for Vps15^{f/f}, n = 4 for AlbCre⁺; Vps15^{f/f}, †P < .01, ‡P < .001; vs Vps15^{f/f}, two-tailed, unpaired Student's *t* test). D, Corticosterone levels in the liver tissue and in plasma of mice collected as in (A), analysed by LC-MS/MS and presented as peak area (arbitrary units). Data are means ± SEM (n = 5 for Vps15^{f/f}, n = 7 for AlbCre⁺; Vps15^{f/f}, †P < .01; vs Vps15^{f/f}, two-tailed, unpaired Student's *t* test). E, Immunoblot analysis of nuclear extracts of livers collected as in (A) using indicated antibodies. Densitometric analyses of protein levels normalized to β-catenin levels presented as folds over Vps15^{f/f}. Data are means ± SEM (n = 4 for Vps15^{f/f}, n = 4 for AlbCre⁺; Vps15^{f/f}, †P < .01; vs Vps15^{f/f}, two-tailed, unpaired Student's *t* test). F, Immunoprecipitation of GR from total protein extracts of livers of mice collected as in (A) followed by immunoblot with anti-ubiquitin antibodies. Densitometric analyses of ubiquitination levels normalized to GR levels presented as folds over Vps15^{f/f}. Data are means ± SEM (n = 3 for Vps15^{f/f}, n = 3 for AlbCre⁺; Vps15^{f/f}, †P < .01; vs Vps15^{f/f}, two-tailed, unpaired Student's *t* test)

Akt signalling and increased GR protein turnover by poly-ubiquitination. We and others have previously demonstrated that due to inhibited endosomal trafficking and blocked lysosomal degradation of insulin receptor, Vps15-LKO mice show persistent activation of Akt signalling.^{8,9} Two Akt substrates were reported to act upstream of GR. Namely, GSK3 β / α was reported as a kinase of Ser211 while Mdm2 is a known E3 ubiquitin ligase of GR to promote its polyubiquitination for proteasomal degradation.^{20,34,35} Phosphorylation of Mdm2 by Akt stimulates its nuclear localization and E3 ligase activity.^{36,37} At the same time, phosphorylation of GSK3 by Akt inhibits its protein kinase activity.³⁸ To interfere with nuclear GR, Akt signalling should reside in nucleus and, consistently, we found increased phospho-Ser473Akt1, a mark of its activation, as well as upregulated phospho-Ser166Mdm2 and phospho-Ser9/21 GSK3 β / α in liver nuclear extracts of Vps15-LKO mice (Figure 4E). Interestingly, increased phosphorylation of Ser473 in Akt1 was also evident in the livers of mice upon acute depletion of Vps15 (Figure S1B). Given that poly-ubiquitination and subsequent proteasomal degradation control GR protein turnover, we tested whether ubiquitination of GR is impacted by chronic inactivation of class 3 PI3K. Immunoprecipitation of GR followed by immunoblot with anti-ubiquitin antibodies demonstrated that in line with its decreased protein levels in Vps15-LKO mice, poly-ubiquitination of GR was significantly augmented in the livers of Vps15 mutants compared with controls (Figure 4F). Increased poly-ubiquitination of GR in the livers of Vps15-LKO mice was accompanied by accumulation of polyubiquitinated proteins in total liver extracts (Figure 4F). The latter is a hallmark of defective proteostasis commonly observed in autophagy mutants.^{39,40-42} Altogether, these findings show positive correlation of increased nuclear Akt1 signalling and GR polyubiquitination in the livers of Vps15-LKO mice.

3 | DISCUSSION

In this work, we demonstrated that chronic inactivation of class 3 PI3K by hepatocyte-specific deletion of its essential regulatory subunit, Vps15, manifests in decreased protein levels of the transcription factor nuclear receptor, GR. We also show that activatory phosphorylation of GR at Ser211 is significantly lower in the livers of Vps15-LKO mice. We demonstrate that fasting or acute administration of DEX, two potent stimuli for GR activation, did not restore expression of GR target genes in Vps15 mutants to the levels observed in the livers of control mice. Finally, we provide the molecular insights into potential mechanisms of GR dysfunction in Vps15 mutants. To this end, we show that

consistent with GR inhibition, the expression of 11 β HSD1 that converts inactive GC precursor into its active corticosterone form, as well as levels of corticosterone are significantly decreased in the livers of Vps15-LKO mice. We also demonstrate that nuclear Akt1 signalling is augmented in the livers of Vps15 mutants. In line with the reported repressive role of Akt on GR activity and protein stability, we observed enhanced polyubiquitination of GR protein in the livers of Vps15-LKO mice. Although GR is reported to activate transcription of autophagy related genes and to promote autophagy,²⁵⁻²⁷ our findings point to unappreciated feedback of class 3 PI3K on GR activity.

In the liver, GC-activated GR activates transcription of a broad range of gene targets involved in glucose and lipid metabolism, bile acid transport, amino acid metabolism, inflammatory pathways and transcriptional regulation.¹² Notably, our findings suggest that inactivation of class 3 PI3K impacts general transcriptional activity of GR, consistent with decreased protein expression of nuclear GR and its phosphorylated at Ser211 form in the livers of Vps15 mutants. However, potential selectivity is suggested by lower magnitude of transcriptional induction in response to DEX treatment for *Dgat2*, *Isig1* and *Tat* genes in the livers of Vps15 mutants compared with controls. Future works using an unbiased GR ChIP-Seq approach in class 3 PI3K mutants will provide a wider view of its gene targets and might reveal specific GR gene signatures selectively affected by class 3 PI3K activation or inhibition. Notably, specific inhibition of autophagy or endocytic trafficking in hepatocytes, two processes controlled by class 3 PI3K, could point to molecular mechanisms upstream of GR transcriptional activation in the liver.

Our study, although descriptive, provides a few molecular insights into how class 3 PI3K might control GR transcriptional activity. First, we show that class 3 PI3K might control GR ligand levels, possibly by promoting C/EBP β expression. C/EBP β is a transcription factor of 11 β HSD1, which is essential for production of active GC in the liver. Moreover, C/EBP β has dual actions on GR, both activating and repressing transcription of its targets by changing chromatin accessibility in GR binding sites.⁴³ Thus, given that Vps15-LKO mutants showed decreased transcripts levels of C/EBP α and C/EBP β , inhibited transcriptional activity of GR might be due to defects in steroid hormone metabolism as well as lower expression of GR transcriptional co-factors. Second, expression of chaperones and Fabps could represent another layer of GR control by class 3 PI3K. We found decreased levels of cytosolic and increased nuclear levels of Hsp90 in the livers of Vps15-LKO mice. These could be the consequence of defective proteostasis in cells lacking class 3 PI3K because of inactive lysosomal degradation and an overloaded proteasome degradation. The latter is consistent with observations in

autophagy mutants and backed by findings of accumulated polyubiquitinated proteins in liver extracts of Vps15-LKO mice (Figure 4F).³⁹⁻⁴² Yet, there is no consensus on the impact of the nuclear Hsp90 on GR transcriptional activity. Hsp90 was reported to stabilize the association of ligand-bound GR to DNA and to stimulate its transcriptional activity.⁴⁴ Another report demonstrated that nuclear Hsp90 inhibited GR transcription by reducing its association with GC response elements at chromatin.³¹ Thus, future works should clarify functional impacts of class 3 PI3K on nuclear Hsp90 turnover and its contribution to GR regulation in the liver. Moreover, recent pre-print study suggested that nuclear Fabp1 might act as a co-activator of GR, similar to its effect on nuclear receptor PPAR α ³² (<https://doi.org/10.1101/2021.07.02.450968>). It will be interesting to test whether the rescue of nuclear Fabp1 levels could reactivate GR transcription in Vps15-depleted hepatocytes. Finally, given that class 3 PI3K activates selective autophagy of transcriptional repressors, Hdac3 and NcoR1,^{10,11} it is tempting to propose that their inhibition might restore GR function in Vps15 mutants. These mechanistic experiments may reveal the molecular interconnection of autophagy and transcriptional control of nuclear receptors in physiological fasting-feeding cycles.

Transcriptional activity of GR is controlled by phosphorylation at Ser residues in the N-terminal domain (S113, S134, S141, S143, S203, S211, S226, S404).⁴⁵ We focused on Ser211 phosphorylation which is strongly linked to full GC-induced activation of GR.^{29,45} Our analyses show that levels of phospho-Ser211GR are decreased and cannot be recovered by acute DEX treatment in Vps15-LKO mice. This observation could be due to low GR protein expression or because class 3 PI3K is required for specific protein kinase/phosphatase activity in hepatocytes. Several protein kinases were reported to phosphorylate GR on Ser211, including MAPK kinases, cyclin-dependent kinases and GSK-3 β .^{12,45,46} Although we cannot totally rule out the defects in AMPK/p38MAPK signalling as the cause of lower phosphorylation of Ser211GR in Vps15-LKO mice, we did not observe differences in their activation (phosphoThr172 AMPK and phosphoThr180/phosphoTyr182 p38) in the livers of fed mutants (data not shown). In our previous study, we reported increased Akt signalling in hepatocytes lacking class 3 PI3K.⁸ Our findings of lower GR phosphorylation in the livers of Vps15-LKO mice are also consistent with repressive functions of activated Akt signalling on GSK3 β / α .³⁸ Furthermore, while Akt and GSK3 are most often discussed as cytosolic signal transduction cascade, both kinases and their different substrates (eg, FoxO1/3a, GR, PGC1a, p300, Mdm2, β -catenin) also function in the nucleus.⁴⁷⁻⁵¹ In addition, as soon as GC-GR activity is induced, an inhibitory feed-back loop for GR repression and degradation is activated to prevent its over-activation.⁵²

One of the E3 ligases that facilitates polyubiquitination for proteasomal degradation of GR is Mdm2.^{20,34,35} It is also a well-known substrate of Akt1 which activates its E3 ligase activity.^{36,37} Thus, our observations of accumulated nuclear phospho-Ser473 Akt1 as well as increased phospho-Ser9/21 GSK3 β / α and phospho-Ser166 Mdm2 in the livers of Vps15 mutants might contribute to GR suppression. Future mechanistic analyses using pharmacological and genetic approaches targeting the Akt1-Mdm2/GSK3 axis in the livers of Vps15-LKO mice will be instrumental to dissect functional crosstalk between class 3 PI3K and GR. Finally, increased proteasomal degradation in the livers of Vps15 mutants might be the cause of higher GR protein turnover. Both inhibition and activation of proteasomal degradation were reported in models of disrupted autophagy, reflecting a complex relationship between these two cellular degradation pathways.^{53,54} Acute depletion of Vps15 in the liver led to decrease in transcript levels of GR target genes without changes in GR protein levels. Thus, it is plausible that defect in GC availability in Vps15-depleted hepatocytes precedes activation of GR proteasomal degradation. In this scenario, decreased protein levels of GR in the livers of Vps15-LKO mice might be secondary to severe proteostasis defects due to chronic inactivation of class 3 PI3K. Altogether, our study opens to future molecular investigations of class 3 PI3K functions upstream of GC-GR transcriptional activity and its function for metabolic control.

4 | MATERIALS AND METHODS

4.1 | Reagents

The following primary antibodies were used: GR (1:1000, Cell Signaling, 3660S); pSer211 GR (1:1000, Cell Signaling, 4161S); Lamp2 (1:1000, Abcam, ab13524); p62 (1:2000, Abnova, H00008878-M01); LC3 (1:500, NanoTools, 0231-100/LC3-5F10); GAPDH (1:2000, Cell Signaling, 5174); β -catenin (1:1000, BD Biosciences, 610 153); HSP90 (1:1000, Proteintech, 13171-1-AP); HSP70 (1:1000, Proteintech, 10995-1-AP); Fabp1 (1:3000, Santa Cruz, sc-374537); Ubiquitin (1:1000, Cell Signaling, 3936); pSer473 Akt1 (1:1000, Cell Signaling, 9018); pSer9/21 GSK3 β / α (1:1000, Cell Signaling, 9331) and pSer166 MDM2 (1:1000, Cell Signaling, 3521). GFP and GFP-Cre adenoviral vectors were described previously.⁵⁵

4.2 | Animals

The Vps15 conditional mutant mouse line was established at the MCI/ICS (Mouse Clinical Institute - Institute

Clinique de la Souris, Illkirch, France) as described.⁵⁶ Liver-specific Vps15 knockout mouse line was generated as described.⁸ Mice were housed in specific pathogen-free conditions. Male mice (6-week-old) were used for the experimentation. Mice were randomly allocated to experimental groups and to ensure statistics analyses and at least three animals were used for each condition (as indicated in figure legends). Animal numbers were chosen to reflect the expected magnitude of response taking into account the variability observed in previous experiments. All animals used in the study were fed ad libitum standard chow diet (Teklad global protein diet; 20% protein, 75% carbohydrate, 5% fat) and kept under 12/12 h (8 AM /8 PM) light on/off cycle. For liver tissue collection, animals were killed between 2 and 4 PM (ZT6-ZT8) unless indicated. For plasma collection, venous blood was collected in ad libitum fed mice at the peak of GC levels (8 PM, ZT12). For fasting experiment, mice were food deprived for 24 h starting at 8 PM (ZT12). For in vivo liver transduction, the adenoviral vectors expressing either GFP or GPF-Cre were administered by retroorbital injection (10^9 /mouse), and the liver tissue was collected ten days later.⁸ All animal studies were performed by authorized users in compliance with ethical regulations for animal testing and research. The study was approved by the Direction Départementale des Services Vétérinaires, Préfecture de Police, Paris, France and the ethical committee of Paris Descartes University (authorization number APAFIS#14968-2017110812164999 v6).

4.3 | Targeted metabolomics

Targeted metabolomics analyses were performed as described.⁵⁷ Briefly, extraction solution used was 50% methanol, 30% ACN and 20% water. The volume of extraction solution added was calculated from the weight of powdered tissue (60 mg/mL) or the volume of the plasma (33ul/ml). After addition of extraction solution, samples were vortexed for 5 min at 4°C, and then centrifuged at $16\ 000 \times g$ for 15 min at 4°C. The supernatants were collected and analysed by liquid chromatography–mass spectrometry using SeQuant ZIC-pHilic column (Merck) for the liquid chromatography separation. Mobile phase A consisted of 20 mM of ammonium carbonate plus 0.1% ammonia hydroxide in water. Mobile phase B consisted of ACN. The flow rate was kept at 200 ml/min, and the gradient was 0 min, 80% of B; 30 min, 20% of B; 31 min, 80% of B; and 45 min, 80% of B. The mass spectrometer (QExactive Orbitrap, Thermo Fisher Scientific) was operated in a polarity switching mode, and metabolites were identified using TraceFinder Software (Thermo Fisher Scientific). The specific peak area is presented.

4.4 | Protein extraction, immunoprecipitation and immunoblotting

To prepare total protein extracts for immunoblot analyses, the liver tissue was powdered in liquid nitrogen, and proteins were extracted in lysis buffer containing 20 mM Tris-HCl (pH 8.0), 5% glycerol, 138 mM NaCl, 2.7 mM KCl, 1% NP-40, 20 mM NaF, 5 mM EDTA, 1× protease inhibitors (Roche), 1× PhosphoStop Inhibitors (Roche). Homogenates were spun at 12,000g for 10 min at 4°C. For immunoprecipitation, 1 mg of total extract was incubated overnight with 5 μ l of anti-GR antibody (Cell Signaling, 3660S). The protein complexes were washed four times with lysis buffer and then eluted by boiling the beads in 1×SDS-sample buffer for 10 min. Protein extracts were resolved by SDS-PAGE on Tris-Bis/MOPS running buffer before transfer onto the PVDF membrane followed by incubation with primary antibodies and HRP-linked secondary antibodies. Immobilon Western Chemiluminescent HRP Substrate (Millipore) was used for the detection. Images were acquired on ChemiDoc™ Imager (Biorad). Nuclear soluble fractions were prepared from 50 mg of frozen tissue of the liver as reported.⁵⁸ Briefly, tissue powder was homogenized in 1 mL of hypotonic buffer (10 mM HEPES pH7.9, 0.5 mM DTT) and incubated on ice for 30 min with vortexing for 10 s every 5 min. Samples were brought to 0.4% NP40 and were incubated on ice for 2 min then vortexed for 10 s. Nuclei were pelleted by centrifugation at 800g for 1min at 4°C. Supernatants were collected as cytosolic fraction. Prior to nuclei extraction, the pellet was washed as follows: three times with 1 mL of hypotonic buffer, once with 1 mL of hypotonic buffer complemented with 14% NP40, three times with 1 mL of hypotonic buffer. Nuclear pellet was re-suspended in 300 μ l of hypertonic buffer (20 mM HEPES pH7.9, 0.5 mM DTT, 0.42 M NaCl, 25% Glycerol, 0.2 mM EDTA pH 8) and incubated on ice for 40 min with vortexing for 10 s every 10 min. Nuclear soluble fraction was recovered by centrifugation at 10,000g for 1 min at 4°C.

4.5 | Real-time quantitative PCR

Total RNA was isolated from the liver tissue using RNAeasy Lipid Tissue Mini Kit (Qiagen). Single-strand complementary DNA was synthesized from 1 μ g of total RNA using 125 ng of random hexamer primers and SuperScript II (Life Technologies). RT-qPCR was performed on QuantStudio 1 (Thermo Fisher Scientific) using an iTaq Universal SYBR Green Supermix (Bio Rad). Relative amounts of mRNA were determined by means of the $2^{-\Delta\Delta CT}$ method, with *eIF2 α* as reference gene and

control treatment or control genotype as the invariant control. Primer sequences are listed in Table S1.

4.6 | Bioinformatic analyses

The source data for microarray analyses are ArrayExpress database (Vps15 depleted liver, E-MTAB-7685)¹⁰ and Gene Expression Omnibus (GR LKO, GSE75682).¹⁹ The gene list of all significantly modified genes (filtered fold change 1.2) was used to compare two data sets. GO analyses of co-regulated genes (upregulated or downregulated) were performed using the Database for Annotation, Visualization and Integrated Discovery (DAVID) V6.8. The functional GO enrichment tests have been made with the R package enrichGO used to create the graphics with the R package clusterProfiler and IDs converted with the R package AnnotationDbi. For GO term analysis, the biological process categories are presented as emaplots.

4.7 | Statistical analysis

Data are shown as means \pm SEM. The unpaired two-tailed Student's *t* test was applied for statistical analysis. Results were considered significant in all experiments at $P < .05$.

ACKNOWLEDGEMENTS

We are grateful to all lab members and the members of INSERM-U1151 for support; to Sophie Berissi (SFR Small animal histology and morphology platform) and Sylvie Fabrega (SFR Viral vector and gene transfer platform) for technical support. This work was supported by grant from Agence Nationale de la Recherche (ANR-JCJC-NUTRISENSPIK-16-CE14-0029) and European Research Council (ERC-2018-CoG-819543) to GP; NH was supported by French National Ministry of Education Fellowship; CA was supported by Boulos Foundation and FRM; Y.S was supported by Japan Society for the Promotion of Science (JSPS) Fellowship DC2.

CONFLICT OF INTEREST

The authors declare no conflict of interests.

AUTHOR CONTRIBUTIONS

YS conducted the analyses, prepared the figures and contributed to the manuscript writing. CA performed in vivo treatments and contributed to expression analyses. IN performed metabolomic analyses. MG performed histopathological evaluation of liver samples in mouse models. NC and NH performed the bioinformatic analyses. TA contributed to data analyses and manuscript writing. GP conceived the study, obtained funding, directed the work,

designed the experiments, analysed the data and wrote the manuscript. All authors discussed the results and commented on the manuscript.

DATA AVAILABILITY STATEMENT

The source data for microarray analyses are ArrayExpress database (Vps15 depleted liver, E-MTAB-7685) and Gene Expression Omnibus (GR LKO, GSE75682).

ORCID

Ivan Nemazanyy  <https://orcid.org/0000-0001-8080-839X>

Ganna Panasyuk  <https://orcid.org/0000-0002-5591-848X>

REFERENCES

1. Kuo T, Lew MJ, Mayba O, et al. Genome-wide analysis of glucocorticoid receptor-binding sites in myotubes identifies gene networks modulating insulin signaling. *Proc Natl Acad Sci USA*. 2012;109:11160-11165. [10.1073/pnas.1111334109](https://doi.org/10.1073/pnas.1111334109)
2. Leis H, Page A, Ramirez A, et al. Glucocorticoid receptor counteracts tumorigenic activity of Akt in skin through Interference with the phosphatidylinositol 3-kinase signaling pathway. *Mol Endocrinol*. 2004;18:303-311. [10.1210/me.2003-0350](https://doi.org/10.1210/me.2003-0350)
3. Piovan E, Yu J, Tosello V, et al. Direct reversal of glucocorticoid resistance by AKT inhibition in acute lymphoblastic leukemia. *Cancer Cell*. 2013;24:766-776. [10.1016/j.ccr.2013.10.022](https://doi.org/10.1016/j.ccr.2013.10.022)
4. Stechschulte LA, Wuescher L, Marino JS, et al. Glucocorticoid receptor β stimulates Akt1 growth pathway by attenuation of PTEN. *J Biol Chem*. 2014;289:17885-17894. [10.1074/jbc.M113.544072](https://doi.org/10.1074/jbc.M113.544072)
5. Hafezi-Moghadam A, Simoncini T, Yang Z, et al. Acute cardiovascular protective effects of corticosteroids are mediated by non-transcriptional activation of endothelial nitric oxide synthase. *Nat Med*. 2002;8:473-479. [10.1038/nm0502-473](https://doi.org/10.1038/nm0502-473)
6. Backer JM. The intricate regulation and complex functions of the Class III phosphoinositide 3-kinase Vps34. *Biochem J*. 2016;473:2251-2271. [10.1042/BCJ20160170](https://doi.org/10.1042/BCJ20160170)
7. Devereaux K, Dall'Armi C, Alcazar-Roman A, et al. Regulation of mammalian autophagy by class II and III PI 3-kinases through PI3P synthesis. *PLoS One*. 2013;8:e76405. [10.1371/journal.pone.0076405](https://doi.org/10.1371/journal.pone.0076405)
8. Nemazanyy I, Montagnac G, Russell RC, et al. Class III PI3K regulates organismal glucose homeostasis by providing negative feedback on hepatic insulin signalling. *Nat Commun*. 2015;6:8283. [10.1038/ncomms9283](https://doi.org/10.1038/ncomms9283)
9. Bilanges B, Alliouachene S, Pearce W, et al. Vps34 PI 3-kinase inactivation enhances insulin sensitivity through reprogramming of mitochondrial metabolism. *Nat Commun*. 2017;8:1804. [10.1038/s41467-017-01969-4](https://doi.org/10.1038/s41467-017-01969-4)
10. Iershov A, Nemazanyy I, Alkhoury C, et al. The class 3 PI3K coordinates autophagy and mitochondrial lipid catabolism by controlling nuclear receptor PPAR α . *Nat Commun*. 2019;10:1566. [10.1038/s41467-019-09598-9](https://doi.org/10.1038/s41467-019-09598-9)
11. Saito T, Kuma A, Sugiura Y, et al. Autophagy regulates lipid metabolism through selective turnover of NCoR1. *Nat Commun*. 2019;10:1567. [10.1038/s41467-019-08829-3](https://doi.org/10.1038/s41467-019-08829-3)

12. Kadmiel M, Cidlowski JA. Glucocorticoid receptor signaling in health and disease. *Trends Pharmacol Sci.* 2013;34:518-530. [10.1016/j.tips.2013.07.003](https://doi.org/10.1016/j.tips.2013.07.003)
13. Hollenberg SM, Weinberger C, Ong ES, et al. Primary structure and expression of a functional human glucocorticoid receptor cDNA. *Nature.* 1985;318:635-641. [10.1038/318635a0](https://doi.org/10.1038/318635a0)
14. Ratman D, et al. Chromatin recruitment of activated AMPK drives fasting response genes co-controlled by GR and PPARalpha. *Nucleic Acids Res.* 2016;44:10539-10553. [10.1093/nar/gkw742](https://doi.org/10.1093/nar/gkw742)
15. Bougarne N, et al. PPARalpha blocks glucocorticoid receptor alpha-mediated transactivation but cooperates with the activated glucocorticoid receptor alpha for transrepression on NF-kappaB. *Proc Natl Acad Sci USA.* 2009;106:7397-7402. [10.1073/pnas.0806742106](https://doi.org/10.1073/pnas.0806742106)
16. Tataranni PA, Larson DE, Snitker S, et al. Effects of glucocorticoids on energy metabolism and food intake in humans. *Am J Physiol.* 1996;271:E317-E325. [10.1152/ajpendo.1996.271.2.E317](https://doi.org/10.1152/ajpendo.1996.271.2.E317)
17. Rahimi L, Rajpal A, Ismail-Beigi F. Glucocorticoid-Induced Fatty Liver Disease. *Diabetes Metab Syndr Obes.* 2020;13:1133-1145. [10.2147/DMSO.S247379](https://doi.org/10.2147/DMSO.S247379)
18. Arlt W, Stewart PM. Adrenal corticosteroid biosynthesis, metabolism, and action. *Endocrinol Metab Clin North America.* 2005;34:293-313. [10.1016/j.ecl.2005.01.002](https://doi.org/10.1016/j.ecl.2005.01.002)
19. He B, Cruz-Topete D, Oakley RH, Xiao X, Cidlowski JA. Human glucocorticoid receptor β regulates gluconeogenesis and inflammation in mouse liver. *Mol Cell Biol.* 2015;36:714-730. [10.1128/mcb.00908-15](https://doi.org/10.1128/mcb.00908-15)
20. Patt M, Gysi J, Faresse N, Cidlowski JA, Odermatt A. Protein phosphatase 1 alpha enhances glucocorticoid receptor activity by a mechanism involving phosphorylation of serine-211. *Mol Cell Endocrinol.* 2020;518: [10.1016/j.mce.2020.110873](https://doi.org/10.1016/j.mce.2020.110873)
21. Denis M, Poellinger L, Wikstöm AC, Gustafsson JA. Requirement of hormone for thermal conversion of the glucocorticoid receptor to a DNA-binding state. *Nature.* 1988;333:686-688. [10.1038/333686a0](https://doi.org/10.1038/333686a0)
22. Vandevyver S, Dejager L, Libert C. On the trail of the glucocorticoid receptor: into the nucleus and back. *Traffic.* 2012;13:364-374. [10.1111/j.1600-0854.2011.01288.x](https://doi.org/10.1111/j.1600-0854.2011.01288.x)
23. Kotelevtsev Y, et al. 11beta-hydroxysteroid dehydrogenase type 1 knockout mice show attenuated glucocorticoid-inducible responses and resist hyperglycemia on obesity or stress. *Proc Natl Acad Sci USA.* 1997;94:14924-14929. [10.1073/pnas.94.26.14924](https://doi.org/10.1073/pnas.94.26.14924)
24. Seckl JR, Walker BR. Minireview: 11beta-hydroxysteroid dehydrogenase type 1- a tissue-specific amplifier of glucocorticoid action. *Endocrinology.* 2001;142:1371-1376. [10.1210/endo.142.4.8114](https://doi.org/10.1210/endo.142.4.8114)
25. Xia X, Kar R, Gluhak-Heinrich J, et al. Glucocorticoid-induced autophagy in osteocytes. *J Bone Miner Res.* 2010;25:2479-2488. [10.1002/jbmr.160](https://doi.org/10.1002/jbmr.160)
26. Troncoso R, Paredes F, Parra V, et al. Dexamethasone-induced autophagy mediates muscle atrophy through mitochondrial clearance. *Cell Cycle.* 2014;13:2281-2295. [10.4161/cc.29272](https://doi.org/10.4161/cc.29272)
27. Deng J, Guo Y, Yuan F, et al. Autophagy inhibition prevents glucocorticoid-increased adiposity via suppressing BAT whitening. *Autophagy.* 2020;16:451-465. [10.1080/15548627.2019.1628537](https://doi.org/10.1080/15548627.2019.1628537)
28. Hinds TD Jr, et al. Discovery of glucocorticoid receptor-beta in mice with a role in metabolism. *Mol Endocrinol.* 2010;24:1715-1727. [10.1210/me.2009-0411](https://doi.org/10.1210/me.2009-0411)
29. Chen W, Dang T, Blind RD, et al. Glucocorticoid receptor phosphorylation differentially affects target gene expression. *Mol Endocrinol.* 2008;22:1754-1766. [10.1210/me.2007-0219](https://doi.org/10.1210/me.2007-0219)
30. Hossain M, Williams S, Ferguson L, et al. Heat shock proteins accelerate the maturation of brain endothelial cell glucocorticoid receptor in focal human drug-resistant epilepsy. *Mol Neurobiol.* 2020;57:4511-4529. [10.1007/s12035-020-02043-9](https://doi.org/10.1007/s12035-020-02043-9)
31. Kang KI, Meng X, Devin-Leclerc J, et al. The molecular chaperone Hsp90 can negatively regulate the activity of a glucocorticosteroid-dependent promoter. *Proc Natl Acad Sci USA.* 1999;96:1439-1444. [10.1073/pnas.96.4.1439](https://doi.org/10.1073/pnas.96.4.1439)
32. Hughes MLR, Liu B, Halls ML, et al. Fatty acid-binding proteins 1 and 2 differentially modulate the activation of peroxisome proliferator-activated receptor α in a ligand-selective manner. *J Biol Chem.* 2015;290:13895-13906. [10.1074/jbc.M114.605998](https://doi.org/10.1074/jbc.M114.605998)
33. Esteves CL, Kelly V, Bégay V, et al. Regulation of adipocyte 11 β -hydroxysteroid dehydrogenase type 1 (11 β -HSD1) by CCAAT/enhancer-binding protein (C/EBP) β isoforms, LIP and LAP. *PLoS One.* 2012;7:e37953. [10.1371/journal.pone.0037953](https://doi.org/10.1371/journal.pone.0037953)
34. Sengupta S, Wasyluk B. Ligand-dependent interaction of the glucocorticoid receptor with p53 enhances their degradation by Hdm2. *Genes Dev.* 2001;15:2367-2380. [10.1101/gad.202201](https://doi.org/10.1101/gad.202201)
35. Kinyamu HK, Archer TK. Estrogen receptor-dependent proteasomal degradation of the glucocorticoid receptor is coupled to an increase in mdm2 protein expression. *Mol Cell Biol.* 2003;23:5867-5881. [10.1128/mcb.23.16.5867-5881.2003](https://doi.org/10.1128/mcb.23.16.5867-5881.2003)
36. Mayo LD, Donner DB. A phosphatidylinositol 3-kinase/Akt pathway promotes translocation of Mdm2 from the cytoplasm to the nucleus. *Proc Natl Acad Sci USA.* 2001;98:11598-11603. [10.1073/pnas.181181198](https://doi.org/10.1073/pnas.181181198)
37. Zhou BP, Liao Y, Xia W, et al. HER-2/neu induces p53 ubiquitination via Akt-mediated MDM2 phosphorylation. *Nat Cell Biol.* 2001;3:973-982. [10.1038/ncb1101-973](https://doi.org/10.1038/ncb1101-973)
38. Cross DA, Alessi DR, Cohen P, Andjelkovich M, Hemmings BA. Inhibition of glycogen synthase kinase-3 by insulin mediated by protein kinase B. *Nature.* 1995;378:785-789. [10.1038/378785a0](https://doi.org/10.1038/378785a0)
39. Pankiv S, Clausen TH, Lamark T, et al. p62/SQSTM1 binds directly to Atg8/LC3 to facilitate degradation of ubiquitinated protein aggregates by autophagy. *J Bio Chem.* 2007;282:24131-24145. [10.1074/jbc.M702824200](https://doi.org/10.1074/jbc.M702824200)
40. Riley BE, Kaiser SE, Shaler TA, et al. Ubiquitin accumulation in autophagy-deficient mice is dependent on the Nrf2-mediated stress response pathway: a potential role for protein aggregation in autophagic substrate selection. *J Cell Biol.* 2010;191:537-552. [10.1083/jcb.201005012](https://doi.org/10.1083/jcb.201005012)
41. Komatsu M, et al. Impairment of starvation-induced and constitutive autophagy in Atg7-deficient mice. *J Cell Biol.* 2005;169:425-434.
42. Komatsu M, Waguri S, Chiba T, et al. Loss of autophagy in the central nervous system causes neurodegeneration in mice. *Nature.* 2006;441:880-884.
43. Grøntved L, John S, Baek S, et al. C/EBP maintains chromatin accessibility in liver and facilitates glucocorticoid receptor recruitment to steroid response elements. *Embo J.* 2013;32:1568-1583. [10.1038/emboj.2013.106](https://doi.org/10.1038/emboj.2013.106)
44. Kirschke E, Goswami D, Southworth D, Griffin PR, Agard DA. Glucocorticoid receptor function regulated by coordinated action of the Hsp90 and Hsp70 chaperone cycles. *Cell.* 2014;157:1685-1697. [10.1016/j.cell.2014.04.038](https://doi.org/10.1016/j.cell.2014.04.038)

45. Wang Z, Frederick J, Garabedian MJ. Deciphering the phosphorylation “code” of the glucocorticoid receptor in vivo. *J Biol Chem*. 2002;277:26573-26580. [10.1074/jbc.M110530200](https://doi.org/10.1074/jbc.M110530200)
46. Nader N, Ng SSM, Lambrou GI, et al. AMPK regulates metabolic actions of glucocorticoids by phosphorylating the glucocorticoid receptor through p38 MAPK. *Mol Endocrinol*. 2010;24:1748-1764. [10.1210/me.2010-0192](https://doi.org/10.1210/me.2010-0192)
47. Martelli AM, Tabellini G, Bressanin D, et al. The emerging multiple roles of nuclear Akt. *Biochim Biophys Acta*. 2012;1823:2168-2178. [10.1016/j.bbamcr.2012.08.017](https://doi.org/10.1016/j.bbamcr.2012.08.017)
48. Beurel E, Grieco SF, Jope RS. Glycogen synthase kinase-3 (GSK3): regulation, actions, and diseases. *Pharmacol Ther*. 2015;148:114-131. [10.1016/j.pharmthera.2014.11.016](https://doi.org/10.1016/j.pharmthera.2014.11.016)
49. Zhou X, Zhong Y, Molinar-Inglis O, et al. Location-specific inhibition of Akt reveals regulation of mTORC1 activity in the nucleus. *Nat Commun*. 2020;11:6088. [10.1038/s41467-020-19937-w](https://doi.org/10.1038/s41467-020-19937-w)
50. Laplante M, Sabatini DM. Regulation of mTORC1 and its impact on gene expression at a glance. *J Cell Sci*. 2013;126:1713-1719. [10.1242/jcs.125773](https://doi.org/10.1242/jcs.125773)
51. Cunningham JT, et al. mTOR controls mitochondrial oxidative function through a YY1-PGC-1alpha transcriptional complex. *Nature*. 2007;450:736-740. [10.1038/nature06322](https://doi.org/10.1038/nature06322)
52. Bellingham DL, Sar M, Cidlowski JA. Ligand-dependent down-regulation of stably transfected human glucocorticoid receptors is associated with the loss of functional glucocorticoid responsiveness. *Mol Endocrinol*. 1992;6:2090-2102. [10.1210/mend.6.12.1491690](https://doi.org/10.1210/mend.6.12.1491690)
53. Korolchuk VI, Mansilla A, Menzies FM, Rubinsztein DC. Autophagy inhibition compromises degradation of ubiquitin-proteasome pathway substrates. *Mol Cell*. 2009;33:517-527. [10.1016/j.molcel.2009.01.021](https://doi.org/10.1016/j.molcel.2009.01.021)
54. Wang XJ, Yu J, Wong SH, et al. A novel crosstalk between two major protein degradation systems: regulation of proteasomal activity by autophagy. *Autophagy*. 2013;9:1500-1508. [10.4161/auto.25573](https://doi.org/10.4161/auto.25573)
55. Panasyuk G, et al. PPARgamma contributes to PKM2 and HK2 expression in fatty liver. *Nat Commun*. 2012;3:672. [10.1038/ncomms1667](https://doi.org/10.1038/ncomms1667)
56. Nemazanyy I, Blaauw B, Paolini C, et al. Defects of Vps15 in skeletal muscles lead to autophagic vacuolar myopathy and lysosomal disease. *EMBO Mol Med*. 2013;5:870-890. [10.1002/emmm.201202057](https://doi.org/10.1002/emmm.201202057)
57. Mackay GM, Zheng L, van den Broek NJ, Gottlieb E. Analysis of cell metabolism using LC-MS and isotope tracers. *Methods Enzymol*. 2015;561:171-196. [10.1016/bs.mie.2015.05.016](https://doi.org/10.1016/bs.mie.2015.05.016)
58. Zhang X, Shu L, Hosoi H, Murti KG, Houghton PJ. Predominant nuclear localization of mammalian target of rapamycin in normal and malignant cells in culture. *J Biol Chem*. 2002;277:28127-28134. [10.1074/jbc.M202625200](https://doi.org/10.1074/jbc.M202625200)

SUPPORTING INFORMATION

Additional supporting information may be found in the online version of the article at the publisher’s website.

How to cite this article: Shibayama Y, Alkhoury C, Nemazanyy I, et al. Class 3 phosphoinositide 3-kinase promotes hepatic glucocorticoid receptor stability and transcriptional activity. *Acta Physiol*. 2022;235:e13793. doi:[10.1111/apha.13793](https://doi.org/10.1111/apha.13793)